12A.5 HIGHLIGHTS OF REFRACTIVITY OBSERVATIONS DURING IHOP_2002

Frédéric Fabry and ShinJu Park
McGill University, Montreal, Quebec, Canada

1. BACKGROUND

Refractivity measurements by radar (Fabry et al. 1997) offer us our first glimpse at the 2-D structure of near-surface moisture at the mesoscale. While most moisture measurements until now had been limited to point values and vertical profiles, refractivity measurements allow us to observe the time evolution of moisture field in the same way that radar reflectivity made possible the study of the mesoscale structure of precipitation.

During IHOP_2002, seven weeks of refractivity data were collected using the NCAR S-Pol radar. These confirmed the ability of refractivity to map the air masses and some of their characteristics (Pettet et al. 2003) as well as the potential of refractivity data for research and operational use. In parallel, very few researchers have been exposed to refractivity imagery and know what kind of information one can obtain from it. In this paper, we will showcase some of the measurements made in Oklahoma in an attempt to both demonstrate their value and give potential users a better feel for what to expect.

2. TYPES OF MEASUREMENTS

Refractivity is measured by monitoring the travel time of radar waves between the radar and fixed targets on the ground. Changes in the phase of a fixed target can be linked to slight changes to the speed of light, from which the refractive index n and the refractivity N of air can be inferred. In the troposphere, N is a function of the pressure P (hPa), the temperature T (K), and the vapor pressure e (hPa) following

$$N = 10^6(n-1) = 77.6\frac{P}{T} + 373000\frac{e}{T^2} = N_{dry} + N_{wet}\ .$$

Two types of images were made. The first is the actual field of N. Although the density term N_{dry} is larger than the moisture term N_{wet}, most of the spatial variability observed in N fields is caused by N_{wet}. Therefore, given representative values for P and T, one can use N to derive e and hence the dew point temperature T_d. In the N images to follow, the color scale has two sets of units: one is for refractivity, which is the quantity that is really being measured, and one is for T_d which is being derived using surface temperature and pressure data from the nine surface stations within 60 km of S-Pol.

The second type of image is the scan-to-scan N change map. This map is counter-intuitively more accurate than the N map, and is especially useful to single out regions where dN/dt is changing such as faint boundaries.

At the S-Pol site, ground targets were typically observed up to 30 km range, except towards the NW quadrant where, after a short gap caused by the Beaver River valley, they were seen up to 60 km range. Because N and dN/dt maps are made using ground targets, the data coverage is much smaller than for reflectivity or Doppler velocity. Nevertheless, it is large enough to allow a variety of observations to be made over the seven week period.

3. EXAMPLES OF RESULTS

The top of Figure 1 shows the histogram of refractivity observed as a function of time. It illustrates the diurnal cycle of N data and the range of values being observed at any time, with dark narrow areas corresponding to very uniform conditions and wide or multimodal light areas being indicative of noticeable gradients in moisture within the small data coverage area. Since it covers the whole field experiment, it gives an unbiased view of the refractivity variability over a long period and allows the reader to get a better appreciation of the frequency of occurrence of the examples to follow.

Twelve sets of examples of refractivity imagery are then provided in the bottom part of Figure 1 associated with different signatures in the histogram. Examples cover a wide variety of phenomena: larger scale moisture boundaries such as those associated with fronts (note [5]), drylines and other convergence lines ([4], [12] and [13]), gust fronts and outflows ([8], [10], [11]), or less sharp gradients of unclear origin ([7] and [10]); boundary layer (BL) phenomena such as rolls ([14]), more cellular structures ([1]), and uneven moistening of the BL by surface fluxes ([6]); and finally, nocturnal waves ([9] and [10]). As this list suggests, refractivity data could hence be of considerable interest not only to meteorologists concerned with convection initiation, but also to researchers in boundary layer processes.

4. ACKNOWLEDGEMENTS

The authors thank Joe Vanandel and Bob Rilling from NCAR for their help in adapting the refractivity code on S-Pol and rerunning the analysis post-facto, and Tammy Weckwerth, Crystalline Pettet, and Ned Chamberlain for the many surface stations near S-Pol used in this study.

Corresponding author address: Frédéric Fabry, McGill University, Atmospheric and Oceanic Sciences, Montreal, QC, H3A 2K6, Canada; e-mail: frederic@radar.mcgill.ca

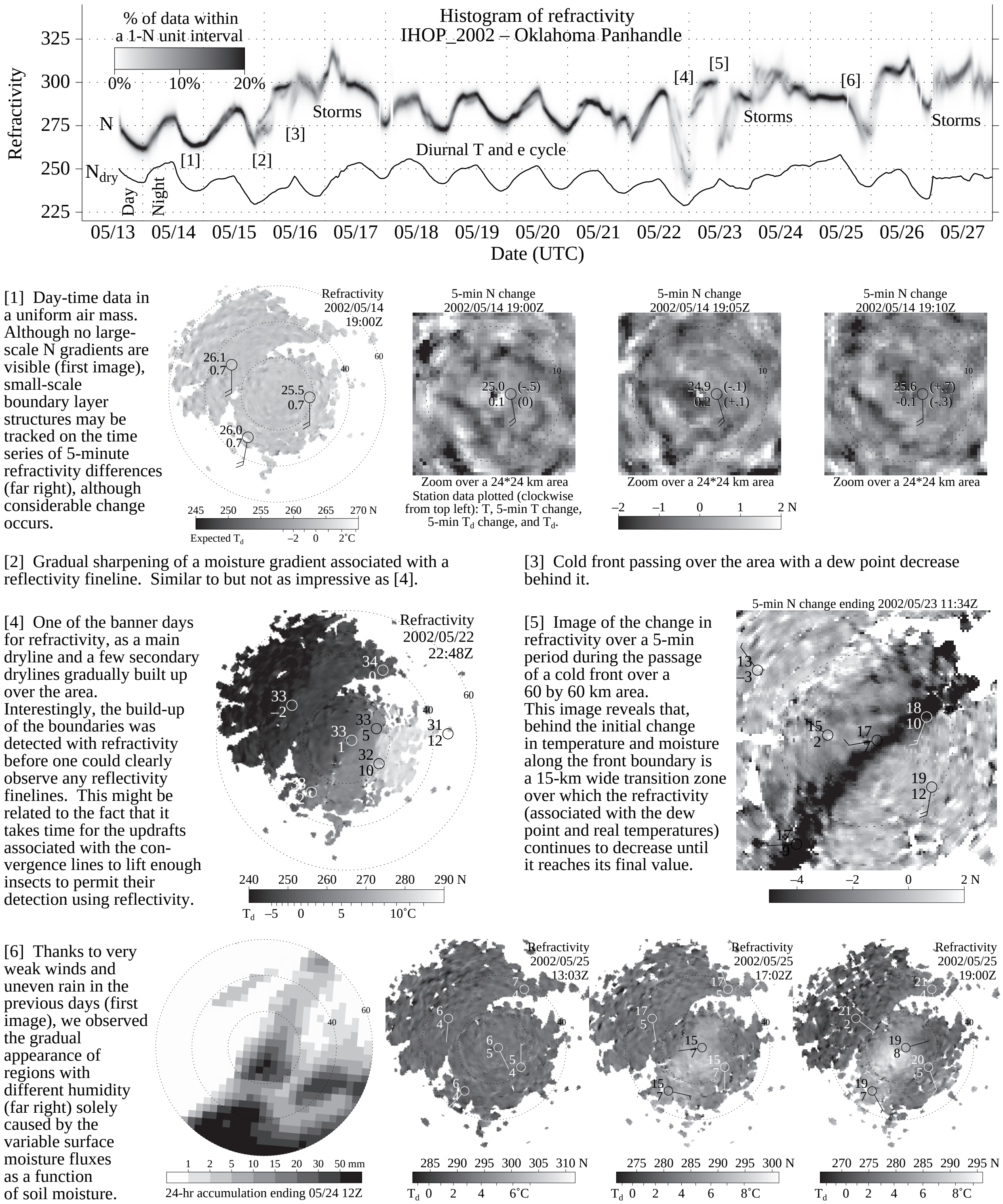

Fig. 1. Top: Histogram of refractivity as a function of time observed by the S-Pol radar in the Oklahoma Panhandle from the 13 May to 25 June 2002. The difference between the N_{dry} curve and the gray shade values is proportional to the amount of moisture measured near the surface.
Bottom: Mini case studies of individual events annotated on the histogram plot. These include a short text description and a variety of radar data (surface refractivity, 5-min surface refractivity change, and PPIs of reflectivity and of Doppler velocity) and surface observations (often plotted on the refractivity maps, sometimes plotted aside in the form of a time series).

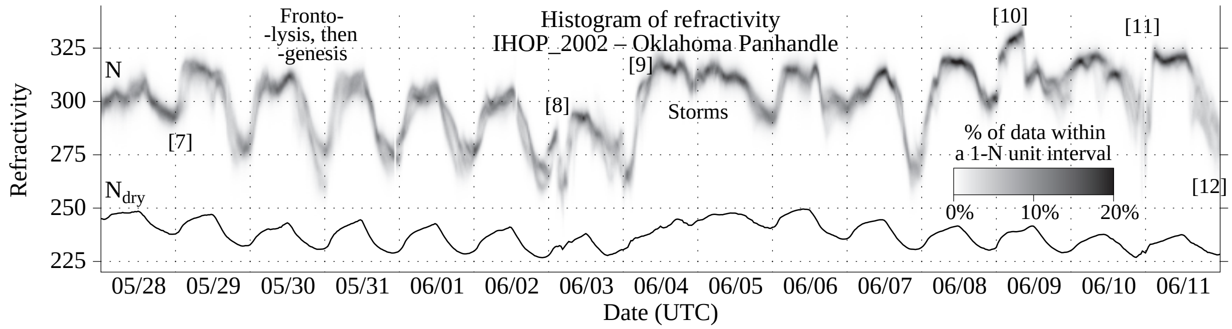

[7] Sudden pulse of surface moisture occurring at the beginning of the night. In this area, nighttime moistening is often associated with the passage of an air-mass boundary coming from the SE early in the night. By contrast, the daytime drying occurs mainly by vertical mixing.
Also note the large difference between N-derived dew point temperatures – representative of data at about 20 m – and the actual surface measurements.

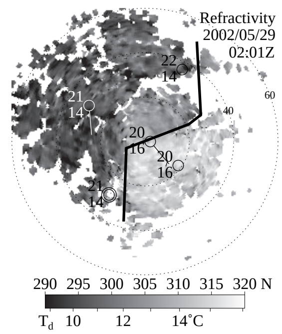

[8] (Multiple?) storm outflow(s) from a line of thunderstorms SW of the radar site. While the reflectivity map shows only one fineline associated with the outflow (solid and dotted line), the refractivity map (right) suggests the presence of multiple boundaries with only an extremely faint refractivity contrast colocated with the reflectivity fineline.
In this case, the outflow is relatively warm and dry; in others (e.g. [11]), it is cool and humid.

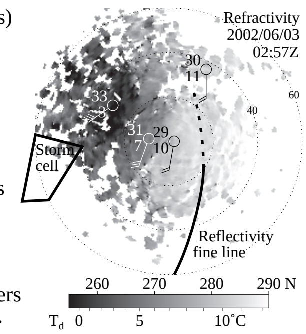

[9] Nighttime bore as seen on (left to right) reflectivity, Doppler velocity and 5-min refractivity change. At this time, the bore is barely detectable on refractivity as pressure waves show some correlation with dew points. Case analyzed by Koch et al. (2003).

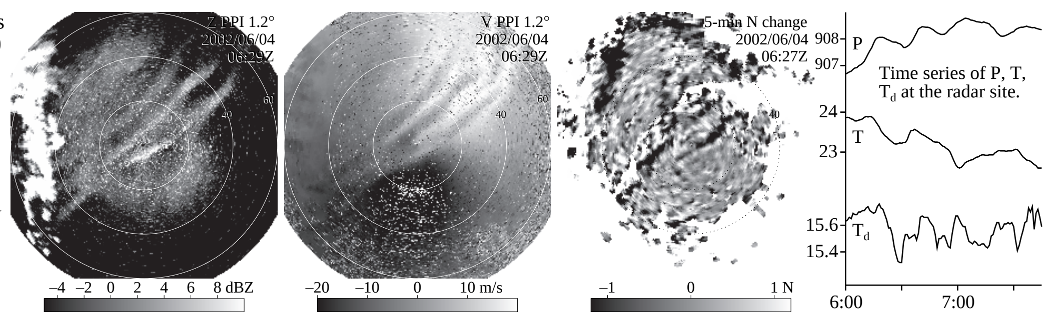

[10] Two examples of refractivity boundaries: a sharp temperature and moisture boundary (caused here by a gust front), and a diffuse moisture transition a few hours later. Both the refractivity change maps and the surface data (far right) show the different nature of the boundaries. The latter example displays hints of a wave structure within it, not an uncommon occurrence for nighttime boundaries.

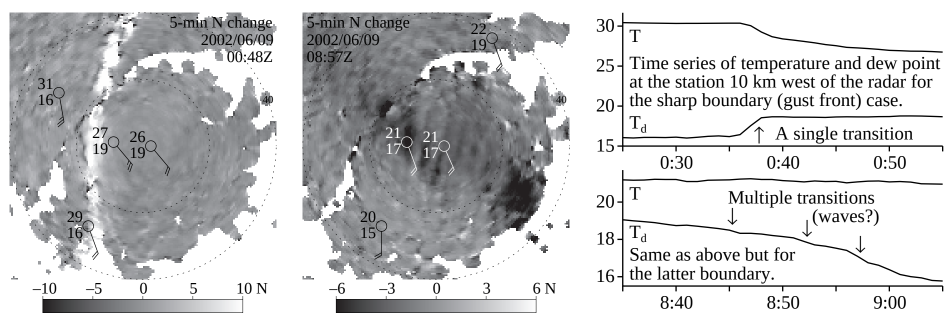

[11] Very high range of refractivity values caused by the presence of multiple storm outflows.
Such conditions cause problems to the algorithm retrieving refractivity fields; hence, data quality is poorer than usual and the field shows considerable fragmentation.

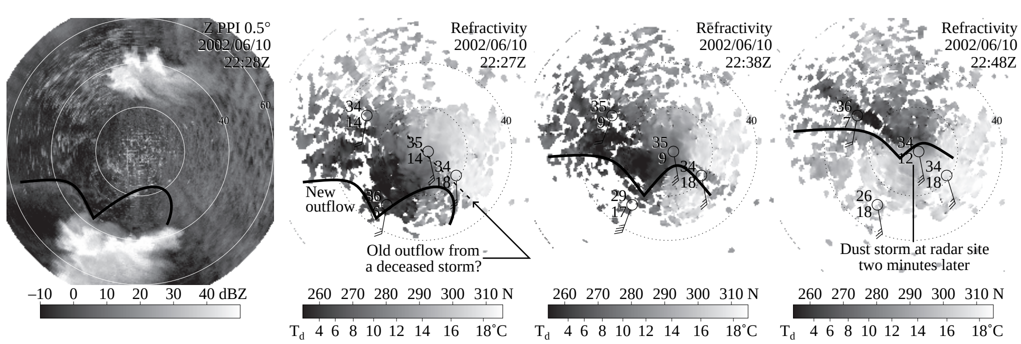

Fig. 1 (cont.)

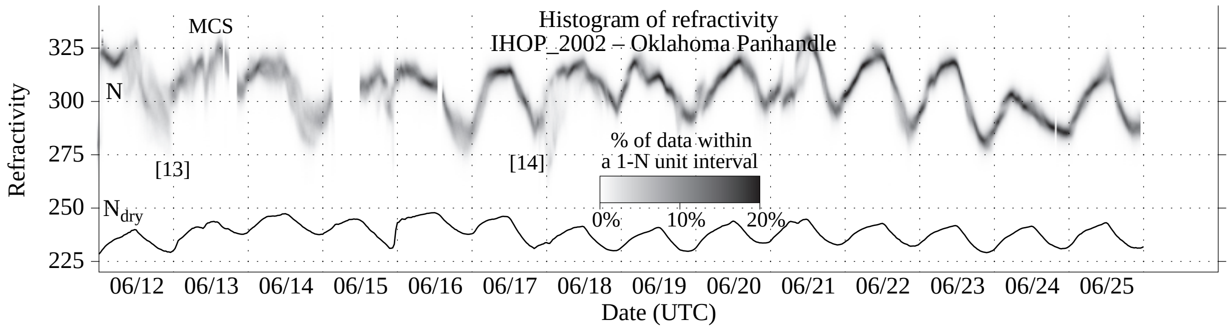

[12] Here, the relatively wide range of refractivity values observed is associated with the presence of a convergence line just NW of the radar site (visible on reflectivity as a fineline (right) as well as on refractivity (far right)). Although clouds poked through the capping inversion (see photo below from S-Pol), no storm initiated.

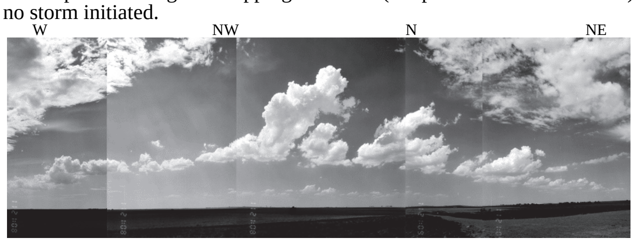

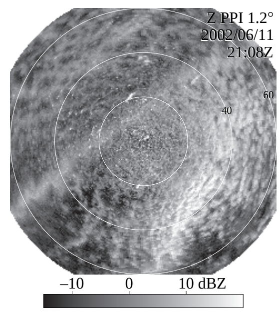

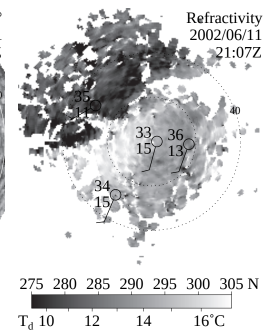

[13] On this day, a weak low pressure system was forming over S-Pol. A persistent slow-moving dry pocket drifted to the southern edge of the refractivity coverage. By 2336Z, a boundary had built up and was moving south (see the refractivity and refractivity change maps on the right). In parallel, a gust front coming from the south can be seen on the reflectivity map (far right) 60 km from the radar. These two boundaries collided 45 min later and a severe thunderstorm initiated 30 km east of S-Pol as a result.

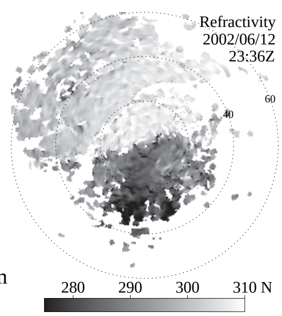

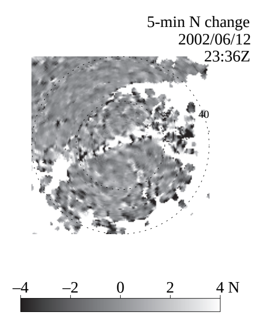

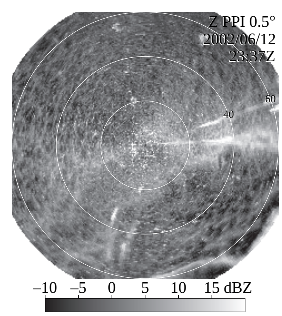

[14] Example of smaller scale variability in refractivity caused by the boundary layer structure on a sunny and windy day. At this time (about 14:00 solar time), BL rolls can be observed on reflectivity (first image). On refractivity (second image), when two images are averaged (19:59 and 20:04) to remove the cross-roll variability, one may observe some along-roll refractivity structure superposed on a stronger larger scale moisture variability. The 5-min refractivity change map (far right), that enhances cross-wind N variability, reveals the presence of cross-roll N structure as well.

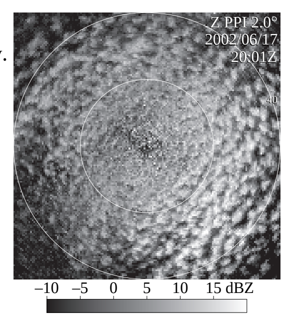

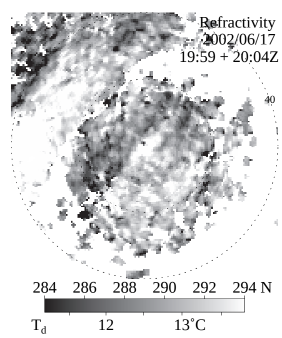

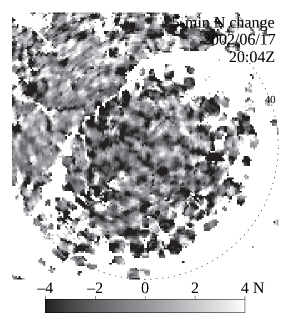

Fig. 1 (cont.)

5. REFERENCES

Fabry F., et al. 1997: On the extraction of near-surface index of refraction using radar measurements of ground targets. *J. Atmos. Oceanic Technol.*, **14**, 978-987.

Koch, S.E., et al. 2003: Multisensor study of a dual bore event observed during IHOP. Preprints, 10th Conf. Mesoscale Processes, Portland OR, paper 14.3.

Pettet, C.R., et al. 2003: An evaluation of the radar refractivity retrieval during IHOP_2002. Preprints, 31st Int. Conf. Radar Meteorology, Seattle WA, paper 10.2.